■ **Materials Science inc. Nanomaterials & Polymers**

# Simple and Rapid One-Step Electrochemical Synthesis of Nanogranular Cu₂O Films

Diego P. Oyarzún,*[a] Martín I. Broens,[b] Omar E. Linarez Pérez,*[b] Manuel López Teijelo,[b] Rafael Islas,[a] and Ramiro Arratia-Perez[a]

In the present work, we report a simple experimental strategy for the one-step electrochemical synthesis of nanogranular Cu₂O films by copper anodization in fluoride-containing ethylene glycol media. Microscopic exploration using field emission scanning electron microscopy (FESEM), atomic force microscopy (AFM) and transmission electron microscopy (TEM), shows the formation of spherical shape grains with sizes ranging from 20 to 40 nm. Raman and X-Ray Photoemission Spectroscopy (XPS) results indicate that only Cu$^I$ oxide is obtained. A band gap energy $E_g = 2.01$ eV is estimated from UV–vis reflectance spectroscopy indicating that an indirect transition mechanism between semiconductor bands takes place. These evidences indicate that the present synthesis of nanogranular Cu₂O films is a promising method for obtaining improved properties of materials for the design of photoelectronic devices.

One of the most interesting purposes in the current nanoscience and nanotechnology research is the optimization of synthesis strategies for tuning the properties of materials at nanoscale dimensions for specific applications. Consequently, a wide variety of metallic, semiconductor and polymeric nanostructures with different size and shape-dependent properties have been obtained.

Among semiconductor materials, Cu₂O has been one of the most studied for applications in photovoltaic cells and electrocatalysis as well as for its microbial activity due to the non-toxic nature, availability, low-cost and narrow band gap ($E_g \approx 1.9$ eV – 2.2 eV).[1–6] In the last years, several reports on the synthesis and characterization of different Cu₂O nanostructures using sol-gel and hydrothermal routes, template assisted growth, electrochemical deposition and anodization, have been published.[3–14]

Particularly, Allam et al[13] reported the synthesis of various Cu₂O nanostructured thin films by anodization of Cu foils in aqueous or ethylene glycol media containing hydroxide, chloride and/or fluoride ions. In aqueous alkaline electrolytes, no stable anodic films on the surface were obtained. Electrodeposited Cu₂O crystallites or dendritic structures were obtained in the presence of chloride ions while in the presence of fluoride ions, uniform nanoporous structures or porous spheroids were achieved. The as-anodized porous nanoarchitectures were composed of a mixture of copper hydroxide and copper oxide phases. On the other hand, for anodization of Cu in ethylene glycol-based electrolytes containing fluoride, leaf-like nanostructures were obtained but no structural film formation was found for the conditions employed. Despite of the variety of nanostructures reported (crystallites, dendritic structures, porous spheroids and leaf-like nanostructures) the synthesis in ethylene glycol media has not been extensively explored. More recently,[14] we have reported that the anodization of copper in alkaline water/ethylene glycol media containing fluoride ions generates nanostructured copper oxide films. By modifying the anodization conditions (fluoride and OH⁻ ions concentration, applied voltage and anodization time), nanofibrillar Cu₂O as well as highly rough nanofibrillar network or nanoporous mixed Cu₂O/CuO films were obtained. Raman and X-ray Photoemission Spectroscopy (XPS) results indicated that in fluoride presence, Cu$^I$ oxide was obtained when anodization takes place applying low voltages at a relatively low OH⁻ concentration. In comparison, the subsequent oxidation to obtain Cu$^{II}$ species (CuO and Cu(OH)₂) was promoted by increasing the OH⁻ content. Additionally, an oxidation reaction scheme was proposed in order to gain a deeper understanding in the preparation of controlled nanostructured copper oxide films.

On the other hand, several disadvantages in the applicability of some of the reported synthesis procedures are the use of special electrolytes, chemicals, surfactants or thermic post-treatments. Overcoming these drawbacks, the electrochemical anodizing technique represents a simple and low-cost method that has been widely applied for many metals. Besides, this method offers a potential control over the nanostructures morphology by changing the anodization parameters such as anodization voltage, temperature, solvent and electrolytic composition.

Based on the above-mentioned reports, we propose a simple and rapid one-step electrochemical strategy of synthesis of nanogranular Cu₂O films by copper anodization in fluoride-containing ethylene glycol media. Microscopic exploration was performed by field emission scanning electron microscopy (FESEM), atomic force microscopy (AFM) and transmission

[a] Dr. D. P. Oyarzún, Dr. R. Islas, Prof. R. Arratia-Perez
Center of Applied Nanosciences (CANS), Facultad de Ciencias Exactas, Universidad Andrés Bello, Avenida República 275, Santiago, Chile
E-mail: diego.oyarzun@unab.cl

[b] M. I. Broens, Dr. O. E. Linarez Pérez, Prof. M. López Teijelo
Instituto de Investigaciones en Fisicoquímica de Córdoba (INFIQC), Facultad de Ciencias Químicas, Universidad Nacional de Córdoba, Haya de la Torre y Medina Allende, 5000 Córdoba, Argentina
E-mail: olinarez@unc.edu.ar

🖥 Supporting information for this article is available on the WWW under https://doi.org/10.1002/slct.201703128

electron microscopy (TEM). On the other hand, Raman, X-Ray Photoemission Spectroscopy (XPS) and UV-vis reflectance techniques were employed for the chemical and spectroscopic analysis.

One-step copper anodization method was explored at 5 °C applying 10 V during 15 min in 0.1 M KOH, 99%v/v ethylene glycol + 1%v/v $H_2O$ electrolytic baths containing different $NH_4F$ content as detailed in the Experimental section (see Supporting Information). Potentiostatic $j/t$ profiles recorded during anodization (Figure 1) show three current stages as the time

a)



b)
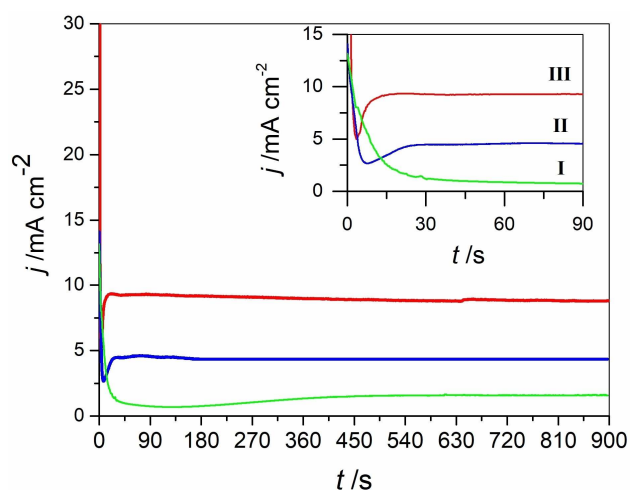


**Figure 1.** Potentiostatic current/time ($j/t$) profiles obtained during anodization of Cu foils for different $NH_4F$ contents: 0.1% w/v (I), 0.2% w/v (II) and 1% w/v $NH_4F$ (III). Applied potential ($E_{ap}$) = 10 V; 5 °C.

increases. Initially, the density current is high due to the copper active dissolution but rapidly decreases indicating the growth of a passivating film, and afterward reaches a minimum that shifts to lower times as fluoride concentration increases. Then, current increases again and finally attains an approximately constant value, which is higher as the fluoride concentration increases. This behavior can be related to the generation of highly porous and/or rough surfaces, which correlates well with the conduct found during anodization of other metals such as titanium performed in similar electrolytes and conditions.[15]

Morphology inspection by AFM (Figure 2), FESEM and TEM (Figure 3), was also performed. For an anodized sample prepared in bath III, top view AFM image (Figure 2a) shows a surface composed by discrete nanograins with an average diameter of 30 ± 10 nm (Figure 2b). Both, cross-section analysis (Figure 2c) and the estimated RMS = 54 nm value indicate that the surface is highly-rough. Additionally, Figure 3 shows FESEM images for anodized copper films and TEM micrographs for aqueous dispersions of nanograins obtained after ultrasound treatment of the anodized samples prepared in electrolytic baths I (Figure 3a,c) and III (Figure 3b,d). Scanning electronic microscopy results show a similar nanostructuration compared to the AFM observation (Figure 2a), evidencing also the reliability of the use of the AFM technique to characterize the
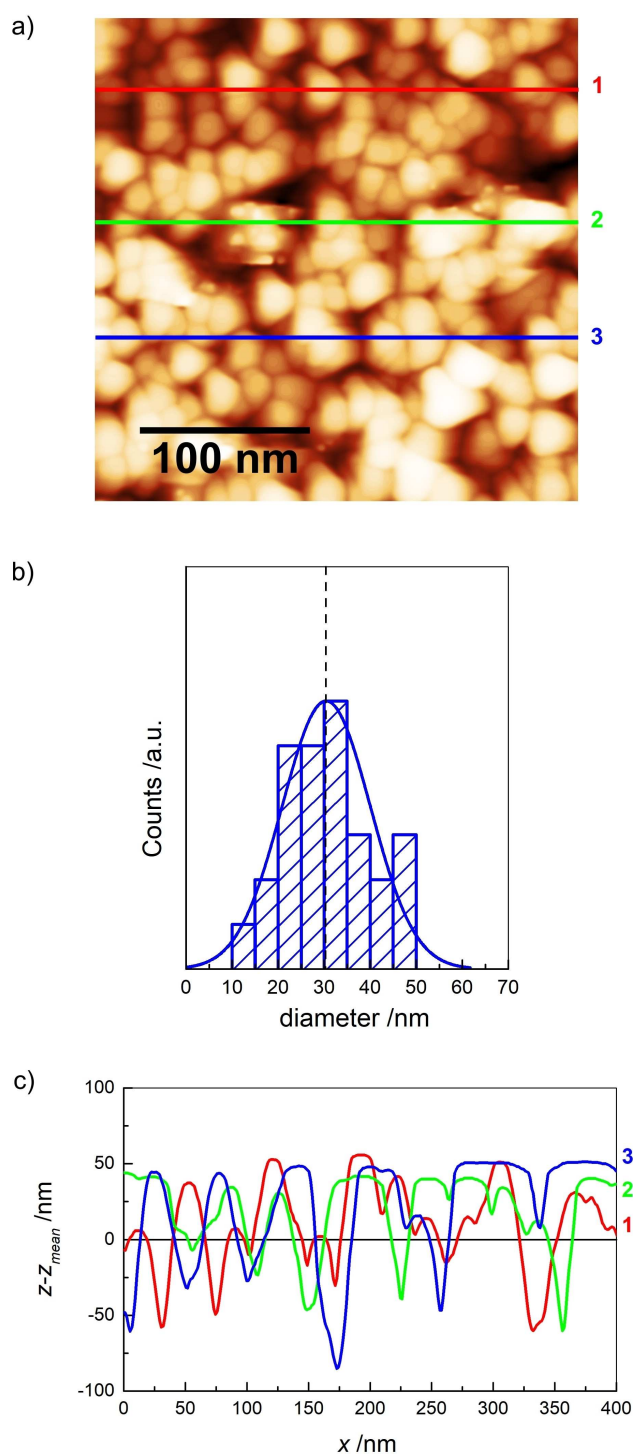
c)



**Figure 2.** 2D AFM image (a) obtained for anodized copper specimens in bath III. b) Nanograin diameter histogram. c) Height cross-section analysis ($z$-$z_{mean}$) in $x$-coordinate corresponding to the lines denoted as 1 (red), 2 (green) and 3 (blue) in (a).

morphology of this material.[16] Statistical analysis for FESEM images (Figure 3e) obtained after the anodization in 0.1% (bath I) and 1% (bath III) fluoride-containing electrolytes indicates that the average diameters are 28 ± 7 nm and 24 ± 6 nm, respectively. The slight decrease in average grain diameter as
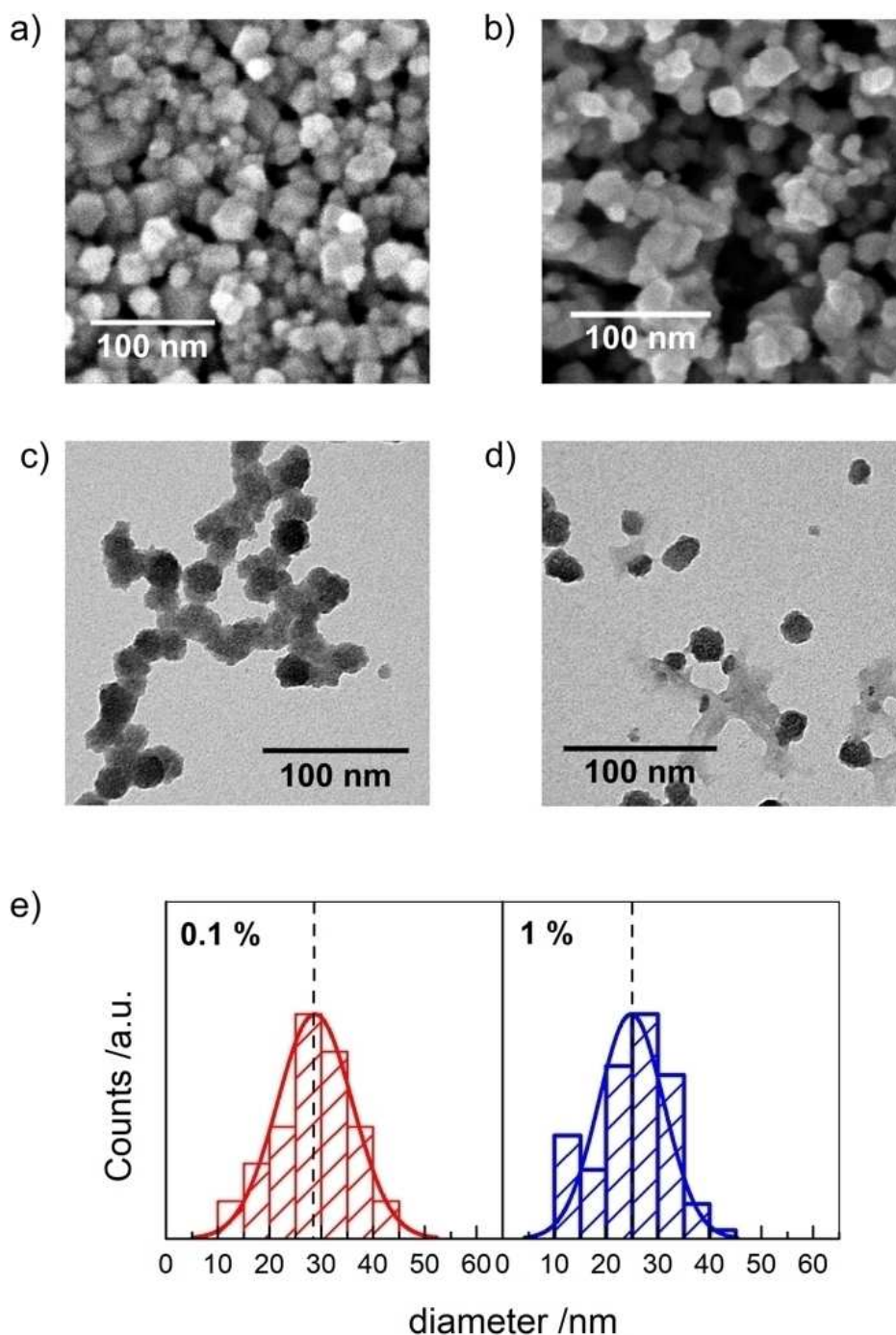
**Figure 3.** FESEM images for anodized copper films (a,b) and TEM micrographs for dispersions of copper specimens (c,d) obtained in bath I (a,c) and III (b,d) (different fluoride percentage content).

the fluoride concentration increases, indicates that fluoride ions influence the surface nanostructuration (see below).

In order to get insight into the chemical copper species present in the nanogranular films, Raman and XPS measurements were performed. Despite of the different current values obtained during the anodization procedure and the bath composition (Figure 1), Raman spectra for the three copper anodized foils do not show significant differences (Figure 4a).

Signals at around 148 cm$^{-1}$, 533 cm$^{-1}$ and 623 cm$^{-1}$ are obtained in all the cases, indicating only the presence of $Cu_2O$ species on the copper surfaces.[17,18] XPS measurements for the anodized copper film obtained in bath III were also performed. The high-resolution Cu 2p spectrum recorded (Figure 4b) shows two well-defined peaks at binding energies of 933.0 eV and 953.0 eV, respectively. For the deconvolution of the spectrum, only one set of signals representing the 2p$_{3/2}$ and
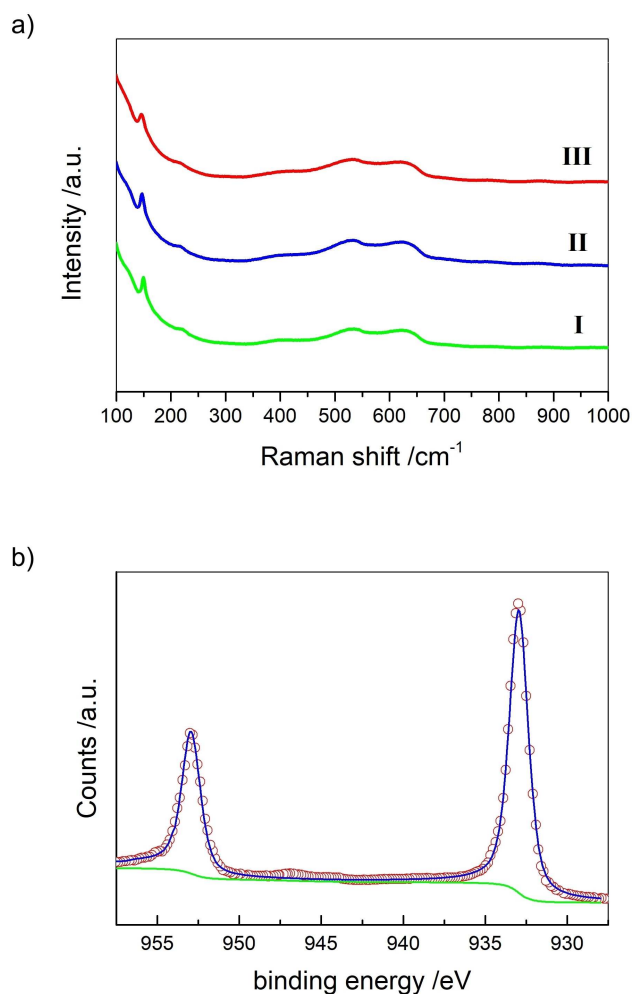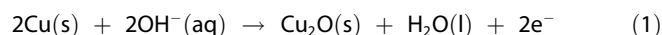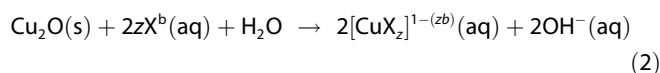
a)



b)



**Figure 4.** a) Raman spectra for anodized Cu foils in the different electrolytic baths (I to III). b) Cu 2p HRXPS spectrum for the anodic film obtained in bath III.

$$Cu_2O(s) + 2zX^b(aq) + H_2O \rightarrow 2[CuX_z]^{1-(zb)}(aq) + 2OH^-(aq) \quad (2)$$

The combination of the experimental conditions employed, mainly applied voltage and time, as well as the passivating properties of the $Cu_2O$ film, determines the rate of process given by Equation 1, while electrolytic bath composition and species concentration, as well as temperature, regulate the $Cu_2O$ anodic film dissolution rate. As a result, the interplay of these two main processes leads to the well-defined copper(I) oxide morphology obtained.

On the other hand, the semiconductor electronic behaviour of the nanogranular $Cu_2O$ films was determined optically by UV-vis spectroscopy, according to the modified Kubelka-Munk method (K–M) described in the literature.[21] This method allows obtaining the band gap energy $E_g$ of the material considering the occurrence of a direct or an indirect transition mechanism between the semiconductor bands. Figure 5 shows the diffuse
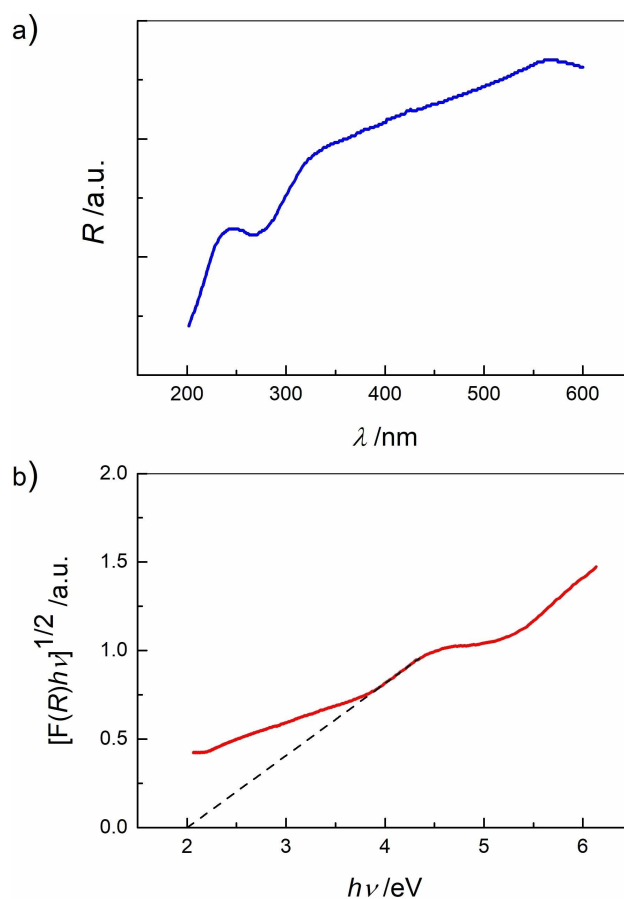
a)



b)



**Figure 5.** Diffuse reflectance spectrum (a) and modified Kubelka-Munk representation (b) for surface obtained in bath III.

$2p_{1/2}$ photoemission doublet was employed. This result as well as the absence of the typical strong $Cu^{II}$ shake-up signal at around 945 eV, indicate that a $Cu^I$ oxide film is obtained.[19] This is in full agreement with Raman results, which indicate that only $Cu_2O$ species are formed for the conditions employed.

Based on the above findings, the synthesis of the copper nanostructures can be described by the occurrence of two main chemical processes during the anodization. First, copper oxidation yielding an anodic $Cu_2O$ film on the copper surface takes place:

$$2Cu(s) + 2OH^-(aq) \rightarrow Cu_2O(s) + H_2O(l) + 2e^- \quad (1)$$

followed by the generation of soluble $Cu^I$ species due to the local dissolution of the $Cu_2O$ film promoted by the different complexing species present in the electrolytic bath (i.e. fluoride, hydroxyl or ammonia) according to:[20]

reflectance spectrum (Figure 5a) and the dependence of the K–M function $[F(R)h\nu]^{1/n}$ on $h\nu$ (Figure 5b). $F(R)$ is calculated as $F(R) = (1-R)^2/2R$, which is proportional to the material extinction

coefficient, $h$ is the Planck constant, $\nu$ the energy frequency and $n$ is an undetermined exponent related to the transition mechanism. Best linear fit in the energy region near to the absorption edge is obtained assuming an exponent value $n = 2$. This result indicates that an indirect allowed electronic transition between valence and conduction bands takes place, which allows obtaining a band gap value $E_g = 2.01$ eV for the nanograined $Cu_2O$ film synthetized. The $E_g$ value obtained is slightly lower than other values previously reported for different $Cu_2O$ nanostructures ($E_g > 2.1$),[6,8,9,21−23] which may indicate that the present synthesis is also a promising method for obtaining copper oxide nanomaterials with improved photoelectric properties.

In summary, we report a simple and rapid experimental strategy for the one-step anodization of copper for obtaining nanogranular $Cu_2O$ films in a fluoride containing non-aqueous electrolytic medium. The present procedure, unlike other known processes for the formation of $Cu_2O$ nanostructures, does not require special electrolytes, chemicals, surfactants and thermic post-treatments. Microscopic exploration using FESEM, AFM and TEM shows spherical shape grains, with mean-size ranging from 20 to 40 nm. Raman and XPS results indicate that only $Cu^I$ oxide is obtained. In addition, according to an indirect transition mechanism between the semiconductor bands, a band gap energy $E_g = 2.01$ eV is estimated from UV−vis reflectance spectra.

### Supporting information summary

Experimental details are described.

### Acknowledgements

### Conflict of Interest

The authors declare no conflict of interest.

[1] S. Sahoo, S. Husale, B. Colwill, Toh-Ming Lu, S. Nayak, P. M. Ajayan, *ACS Nano* **2009**, *12*, 3935−3944.

[2] S. Zhang, C, Liu, X. Liu, H. Zhang, P. Liu, S. Zhang, F. Peng, H. Zhao, *Appl. Microbiol. Biotechnol.* **2012**, *96*, 1201−1207.

[3] H. E. Emam, H. B. Ahmed, T. Bechtold , *Carbohydr. Polym.* **2017**, *165*, 255−265.

[4] G. O. Larrazábal, A. J. Martín, F. Krumeich, R. Hauert, J. Pérez-Ramírez, *ChemSusChem* **2017**, *10*, 1255−1265.

[5] S. Alvarez, S. Ye, P. F. Flowers, B. J. Wiley, *Chem. Mater.* **2015**, *27*, 570 − 573.

[6] H. Rahal, R. Kihal, A. M. Affoune, S. Rahal, *Chin. J. Chem. Eng.* **2018**, *26*, 421−427.

[7] G. S. Theja, R. C. Lowrence, V. Ravi, S. Nagarajan, S. P. Anthony, *Cryst. Eng. Comm* **2014**, *16*, 9866−9872.

[8] P. K. Pagare, A. P. Torane, *Microchim Acta* **2016**, *183*, 2983−2989.

[9] S. Laidoudi, A. Y. Bioud, A. Azizi, G. Schmerber, J. Bartringer, S. Barre, A. Dinia, Semicond. *Sci. Technol.* **2013**, *28*, 115005−115012.

[10] I. S. Brandt, C. A. Martins, C. C. Zoldan, A. D. C. Viegas, J. H. Dias da Silva, A. A. Pasa, *Thin Solid Films* **2014**, *562*, 144−151.

[11] A. Sahaia, N. Goswamia, S. D. Kaushikb, S. Tripathi, *Appl. Surf. Sci.* **2016**, *390*, 974−983.

[12] Yanqun Lv, Baozhu Shi, Xiaofa Su, Lecheng Tian, *Mater. Lett.* **2018**, *212*, 122−125.

[13] N. K. Allam, C. A. Grimes, *Mater. Lett.* **2011**, *65*, 1949−1955.

[14] D. P. Oyarzún, M. López Teijelo, W. Ramos Cervantes, O. E. Linarez Pérez, J. Sánchez, G. del C. Pizarro, G. Acosta, M. Flores, R. Arratia-Pérez, *J. Electroanal. Chem.* **2017**, *807*, 181−186.

[15] D. Kowalski, D. Kim, P. Schmuki, *Nano Today* **2013**, *8*, 235−264.

[16] D. P. Oyarzún, O. E. Linarez Pérez, M. López Teijelo, C. Zúñiga, E. Jeraldo, D. A. Geraldo, R. Arratia-Perez, *Mater. Lett.* **2016**, *165*, 67−70.

[17] J. C. Hamilton, J. C. Farmer, R. J. Anderson, *J. Electrochem. Soc.* **1986**, *133*, 739−745.

[18] S. T. Mayer, R. H. Muller, *J. Electrochem. Soc.* **192**, *139*, 426−434.

[19] I. Platzman, R. Brener, H. Haick y R. Tannenbaum, *J. Phys. Chem. C* **2008**, *112*, 1101−1108.

[20] S. Kotrlý, L. Šůcha in *Handbook of Chemical Equilibria in Analytical Chemistry*, Ellis Horwood Limited, Halsted Press, John Wiley & Sons, New York, **1985**.

[21] R. López, R. Gómez, *J. Sol-Gel Sci. Technol.* **2012**, *61*, 1−7.

[22] J. F. Pierson, A. Thobor-Keck, A. Billard, *Appl. Surf. Sci.* **2003**, *210*, 359−367.

[23] B. K. Meyer, A. Polity, D. Reppin, M. Becker, P. Hering, P. J. Klar, Th. Sander, C. Reindl, J. Benz, M. Eickhoff, C. Heiliger, M. Heinemann, J. Bläsing, A. Krost, S. Shokovets, C. Müller, C. Ronning, *Phys. Status Solidi B* **2012**, *249*, 1487−1509.